

Biofilms formed by the archaeon *Haloferax volcanii* exhibit cellular differentiation and social motility, and facilitate horizontal gene transfer

Chimileski *et al.*

RESEARCH ARTICLE

Open Access

Biofilms formed by the archaeon *Haloferax volcanii* exhibit cellular differentiation and social motility, and facilitate horizontal gene transfer

Scott Chimileski¹, Michael J Franklin² and R Thane Papke^{1*}

Abstract

Background: Archaea share a similar microbial lifestyle with bacteria, and not surprisingly then, also exist within matrix-enclosed communities known as biofilms. Advances in biofilm biology have been made over decades for model bacterial species, and include characterizations of social behaviors and cellular differentiation during biofilm development. Like bacteria, archaea impact ecological and biogeochemical systems. However, the biology of archaeal biofilms is only now being explored. Here, we investigated the development, composition and dynamics of biofilms formed by the haloarchaeon *Haloferax volcanii* DS2.

Results: Biofilms were cultured in static liquid and visualized with fluorescent cell membrane dyes and by engineering cells to express green fluorescent protein (GFP). Analysis by confocal scanning laser microscopy showed that *H. volcanii* cells formed microcolonies within 24 h, which developed into larger clusters by 48 h and matured into flake-like towers often greater than 100 μm in height after 7 days. To visualize the extracellular matrix, biofilms formed by GFP-expressing cells were stained with concanavalin A, DAPI, Congo red and thioflavin T. Stains colocalized with larger cellular structures and indicated that the extracellular matrix may contain a combination of polysaccharides, extracellular DNA and amyloid protein. Following a switch to biofilm growth conditions, a sub-population of cells differentiated into chains of long rods sometimes exceeding 25 μm in length, compared to their planktonic disk-shaped morphology. Time-lapse photography of static liquid biofilms also revealed wave-like social motility. Finally, we quantified gene exchange between biofilm cells, and found that it was equivalent to the mating frequency of a classic filter-based experimental method.

Conclusions: The developmental processes, functional properties and dynamics of *H. volcanii* biofilms provide insight on how haloarchaeal species might persist, interact and exchange DNA in natural communities. *H. volcanii* demonstrates some biofilm phenotypes similar to bacterial biofilms, but also has interesting phenotypes that may be unique to this organism or to this class of organisms, including changes in cellular morphology and an unusual form of social motility. Because *H. volcanii* has one of the most advanced genetic systems for any archaeon, the phenotypes reported here may promote the study of genetic and developmental processes in archaeal biofilms.

Keywords: biofilm, *Haloferax volcanii*, microbial development, archaeal genetics, archaeal biofilm, horizontal gene transfer, amyloid, collective behavior, swarming, haloarchaea

* Correspondence: thane@uconn.edu

¹Department of Molecular and Cell Biology, University of Connecticut, Storrs, Connecticut, USA

Full list of author information is available at the end of the article

Background

The perception of bacteria and archaea as autonomous single-celled organisms is steadily shifting as the capacity to live within structured communities known as biofilms is discovered in species spanning broad taxonomic groups [1–3]. Biofilms are composed of many microbial cells, often of multiple species, held within an extracellular matrix (ECM) [4]. Because biofilms bring cells together in close physical proximity, the process of biofilm formation is coupled with additional social systems and mechanisms fundamental to microbiology, including quorum sensing (and other forms of cell-to-cell communication), horizontal gene transfer (HGT) and the secretion of enzymes that degrade complex material, causing the ECM to act like a kind of shared external digestive system [3,5]. The end result is a community lifestyle whereby cells may benefit from the advantages of enhanced protection from natural eukaryotic predators [6], other antagonistic microbial species, chemicals, antibiotics or immune responses [5,7,8]. Biofilms may aid in nutrient acquisition and storage [5], facilitate accelerated rates of recombination [9,10] and allow for coordinated multicellular behaviors [11–15]. Direct analyses of aquatic ecosystems have led to the realization that a majority of microbial species in nature exist in biofilms [2,16–20].

General features of bacterial biofilms have been revealed through the study of several key model species, including *Pseudomonas aeruginosa*, *Staphylococcus aureus* and *Bacillus subtilis*. Chemical signals and other external factors often regulate the biofilm lifecycle in bacteria, a sequential process typified by initial attachment of planktonic cells, microcolony formation, maturation into larger structures innervated by aqueous pores or channels, and eventual breakdown or dispersal [5,21,22]. Rather than being simple aggregates of many cells, biofilms contain microenvironments with physical and chemical gradients that establish spatial and temporal genetic patterns sometimes leading to differentiation into multiple cell types [23–26]. Many genes involved in the production and maintenance of matrix materials or extracellular polymeric substances (EPSs) have also been identified [5,27–29]. The principal components of bacterial matrices are polysaccharides, extracellular DNA (eDNA) and amyloid protein [5]. The exact composition, physical and chemical properties, and amounts of these components varies in different species and environmental conditions [4].

While biofilm formation is best characterized for bacterial species [30,31], it has been demonstrated in a number of archaeal groups within the phyla Crenarchaeota and Euryarchaeota, such as *Sulfolobus* spp. [32–34], methanogens [30], acidophilic thermoplasmatales [35], the cold-living SM1 strain found in sulfuric springs [36,37] and halophilic archaea [38]. A recent survey of biofilm formation in haloarchaea (i.e., members of the class Halobacteria)

conducted by Fröls and coworkers showed that a majority of tested strains were able to adhere to glass and form biofilms [38]. Species were categorized according to adhesion strength and overall biofilm structure. *Haloferax volcanii* fell within the highest adherence group, and formed large surface associated aggregates, relative to other species, including *Halobacterium salinarum*, which formed smaller micro- and macrocolonies in carpet-like layers [38].

We conducted a physiological analysis of biofilm formation by *H. volcanii* DS2 due to several advantages of using this species as a model for archaeal biofilm formation. The wild-type *H. volcanii* DS2 strain was cultivated from sediment from the Dead Sea in 1975 [39]: it is a relatively fast-growing non-fastidious mesophile, requiring no special equipment to grow in the laboratory [40,41] and was the first archaeon to be artificially transformed [42]. *H. volcanii* DS2 has an available genome sequence [43] and an expanding genetic and proteomic toolbox [42,44–49]. Haloarchaea also undergo promiscuous gene transfer in the environment [50–52] and are excellent species for studying evolutionary processes due to island-like distribution [53–55]. We hypothesize that a cell-to-cell contact-dependent gene transfer mechanism in *H. volcanii* [56–58] may be active when cells are contained within biofilm communities. The available genetic system allowed us to engineer a *H. volcanii* strain expressing GFP for three-dimensional biofilm imaging by confocal laser scanning microscopy (CLSM). Here we characterize key aspects of *H. volcanii* biofilm structural development, composition, dynamics and recombination frequency.

Results

Haloferax volcanii cells develop into structured colony biofilms and static liquid biofilms

Planktonic *H. volcanii* DS2 cells grown in shaking culture (Figure 1A) readily formed biofilms in typical rich media types Hv-YPC and Hv-Ca within several experimental systems that provided a solid plastic or glass substratum. Colony biofilms [7] developed on the surface of polycarbonate filters placed on solid media (Figure 1B) and were cryo-processed and cross-sectioned, exposing a surface structure containing crevices bounded by globular structures (Figure 1B). The greatest level of structural complexity was observed when biofilms were grown in static liquid (SL-biofilms; Figure 1C). Cultivating SL-biofilms within chamber slides and on the surface of borosilicate glass coupons placed in six-well plates permitted direct staining and optimized imaging of delicate biofilm structure that was visible macroscopically (Figure 1C).

We began by examining the development of wild-type *H. volcanii* DS2 biofilms in static liquid using CLSM and the cellular membrane dyes FM 1-43 and CellMask Orange

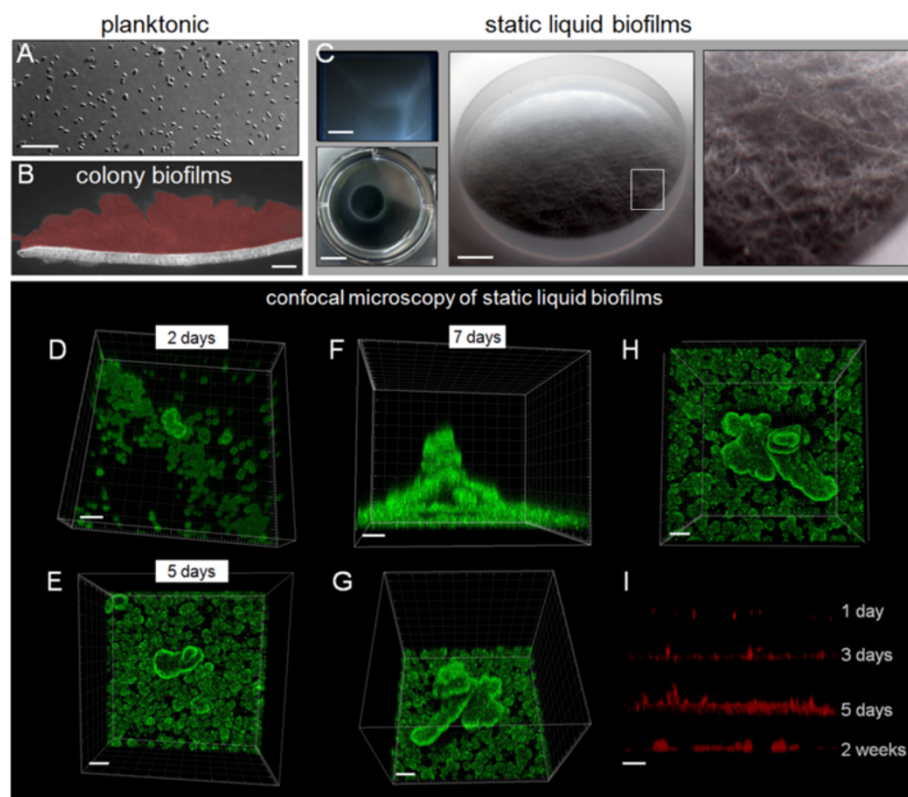


Figure 1 Growth and development of *Haloferax volcanii* static liquid biofilms. (A) Cells within typical shaken culture of *H. volcanii* DS2 under transmitted light. Scale bar equals 10 μ m. (B) Cross section of cryo-processed *H. volcanii* colony biofilm grown on CA medium for 5 days and stained with CellMask Orange (CMO). Scale bar equals 30 μ m. (C) Photographs of SL-biofilms routinely grown and analyzed within chamber slides (top left; scale bar equals 2 mm) and on glass coupons within six-well plates (bottom left; scale bar equals 1 cm). A macroscopic photograph of biofilm growth on a 12.7-mm glass coupon is shown in the center (scale bar equals 2 mm) with an area magnified on the right (shown in white box). (D-H) CLSM of biofilms grown on glass coupons (within a six-well plate in Hv-Ca medium; scale bars equal 30 μ m). Biofilms stained with FM 1-43 were imaged directly in bulk Hv-starve medium using a 63 \times water-immersion objective after 2 days (D), 5 days (E) and 7 days (F-H). (I) Biofilm development shown through orthogonal views of SL-biofilms on glass coupons stained with CMO. CLSM, confocal laser scanning microscopy; CMO, CellMask Orange; SL-biofilm, static liquid biofilm.

(CMO; Figure 1D–I, Additional file 1: Table S1). Circular microcolonies formed within 48 h (Figure 1D), which led to well-defined clusters/aggregates after 5 days (Figure 1E). SL-biofilms reached maturation after 7 days of incubation at 42°C having developed into multi-layer towers with flake-like morphology (Figure 1F,G,H). Large towers were surrounded by a dense layer of smaller clusters or microcolonies and were separated by areas with little or no cell density (Figure 1E–H). Overall structural integrity was maintained as large clusters surrounded by smaller microcolonies for several weeks, although a comparison of orthogonal views of CMO-stained SL-biofilms showed that after 2 weeks the height of most structures was diminished and less of the total surface area was covered with microcolonies (Figure 1I, 2 weeks). Large clusters/towers, like the example shown in Figure 1F,G,H, varied in height and width, with a maximum measured height of 148 μ m.

Microcolonies within biofilms formed by a GFP-expressing *Haloferax volcanii* strain bind stains targeting polysaccharide, DNA and amyloid protein

Several *H. volcanii* strains were engineered to express GFP to study ECM composition with the goal of reinforcing and expanding staining experiments conducted by Fröls and coworkers [38]. Confirmation of GFP expression was first accessed within colonies formed by two GFP-expression strains produced in this study. Colonies formed by the parental *H. volcanii* H1206 strain (Figure 2A; left panel) did not autofluoresce with blue excitation (Figure 2A, center panel), while those formed by the *H. volcanii* H1206(pJAM1020) strain based on the previously developed plasmid pJAM1020 (see Additional file 1: Table S2) [59] showed uniform and high levels of GFP fluorescence (Figure 2A; right panel). An additional GFP-expressing strain *H. volcanii* H1206 (pSC409GFP), containing the same red-shifted *gfp* gene as in pJAM1020 but cloned into the plasmid pTA409,

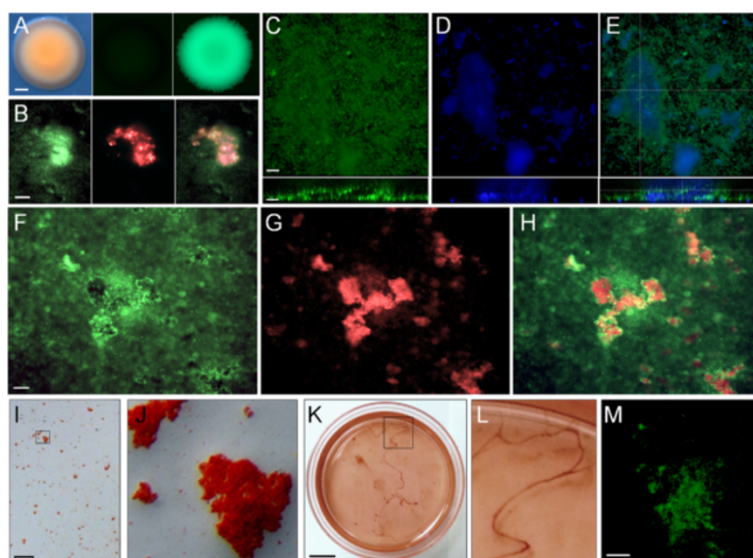


Figure 2 Visualizing the extracellular matrix of *Haloferax volcanii* biofilms. (A) Development of a GFP-expressing strain for use in biofilm visualization: colonies formed by the parental strain *H. volcanii* H1206 under transmitted light (left), under blue excitation (center), and by the strain *H. volcanii* H1206(pJAM1020) under blue excitation (right). Scale bar equals 250 μ m. (B) Seven-day *H. volcanii* H1206(pJAM1020) SL-biofilm stained with concanavalin A-Texas Red collected with blue excitation (left), green excitation (center), and shown as an overlay (right). Scale bar equals 20 μ m. (C,D,E) Top-down projections of a Z-stack for a *H. volcanii* H1206(pJAM1020) SL-biofilm stained with DAPI. (C) GFP signal under blue excitation. (D) DAPI-stained material with violet excitation. (E) Overlay of (C) and (D). Orthogonal views from CLSM analysis are shown below each panel and the plane of the orthoslice is shown in (E). Scale bars equal 20 μ m. (F,G,H) Seven-day *H. volcanii* H1206(pJAM1020) SL-biofilm stained with Congo red with blue excitation (F), and green excitation for CR fluorescence (G), with an overlay of (F) and (G) shown in (H). Scale bar equals 20 μ m. (I) Bright-field view of 7-day CR-stained SL-biofilm within a chamber slide. Scale bar equals 1 mm. Area outlined by black box is shown in (J). (K,L) Ten-day SL-biofilm within Petri dish grown at 25°C in medium containing CR with CR-stained string or web-like structures magnified in (L). Scale bar equals 1 cm. (M) Seven-day H1206 SL-biofilms grown in Hv-YPC medium stained with thioflavin T under blue excitation (top down 3D projection of a Z-stack; scale bar equals 20 μ m). CLSM, confocal laser scanning microscopy; CR, Congo red; DAPI, 4',6-diamidino-2-phenylindole; GFP, green fluorescent protein; SL-biofilm, static liquid biofilm.

produced colonies with GFP signals that differed in both intensity and spatial distribution, resulting in an assortment of patterns of GFP signal within developed colonies (Additional file 1: Figure S1). The H1206(pJAM1020) strain was therefore selected for biofilm compositional studies to ensure stable GFP expression throughout the cellular population.

Cellular clusters visible in GFP-expressing biofilms were colocalized with the signal from a Texas Red conjugate of the lectin concanavalin A (ConA; Figure 2B) and with the DNA binding dye 4',6-diamidino-2-phenylindole (DAPI; Figure 2C,D,E). ConA is known to bind α -mannopyranosyl and α -glucopyranosyl residues within glycoconjugates of haloarchaeal biofilms [38]. DAPI was selected as an extracellular DNA stain for our CLSM study because it is known to stain eDNA preferentially in haloarchaeal biofilms [38]. Fröls and coworkers [38] used three nucleic acid dyes to distinguish between extracellular and intracellular DNA in biofilms formed by *H. volcanii* and additional haloarchaeal strains, and showed that: (a) only acridine orange stained individual live cells, appearing similar our use of the cell permeable nucleic acid dye SYTO 9

(Additional file 1: Figure S2), (b) the signal from DAPI appeared nebulous and granular and was colocalized with microcolonies, (c) simultaneous staining with 7-hydroxy-9H-1-3-dichloro-9,9-dimethylacridin-2-one (DDAO), a nucleic acid dye considered completely impermeable to cells, led to an essentially identical pattern of fluorescence signals, and (d) very few non-viable cells are present within *H. volcanii* biofilms (even after 30 days of incubation), suggesting that the observed DAPI signal was not from dead cells. Our CLSM analysis also showed colocalization of DAPI-stained material with microcolonies and a lack of signal from individual cells. Further three-dimensional reconstruction of DAPI-stained GFP-expressing biofilms revealed that DNA was concentrated in the basal layer of the biofilm and dispersed as plume-like structures at the top of larger towers (Figure 2C,D,E; lower panels).

Larger structures observed in mature biofilms with transmitted light and through GFP fluorescence were also colocalized with the signal from Congo red (CR) and thioflavin T (ThT). These stains are routinely used as characteristic tests for the presence of a wide variety of amyloid proteins, including for diagnosis and study

of disease-causing plaques formed by amyloidosis [60–63], and in many investigations of microbial adhesion and biofilm formation [27,64–71].

Congo red fluorescence (CRF) was used as it has been proposed as the most sensitive and reliable method for amyloid detection when staining with CR [60] and has been applied to biofilm compositional studies [72]. CRF was sharply defined and granular in appearance and was colocalized with the large biofilm cellular clusters and towers shown in Figure 2F,G,H. Overlays where single GFP-producing cells are visible and images of CRF at 600× magnification (Additional file 1: Figure S3) indicated that CR did not stain individual cells. CR-stained biofilm aggregates were also orange-red under transmitted light and were visible macroscopically (Figure 2I–L). Further, green fluorescence signal was detected within ThT-stained mature biofilms formed by a non-GFP strain with blue excitation (Figure 2M; no signal detected in control without ThT staining).

***Haloferax volcanii* undergoes morphological differentiation during biofilm growth**

The implementation of GFP for biofilm visualization led to the unexpected observation of increased variability in length of cellular structures within biofilms compared to planktonic cells (Figure 3). *H. volcanii* DS2 cells are known to be pleomorphic, appearing spherical, disk-like or as short rods 1 to 3 × 2 to 3 μm in size in liquid culture [39] (Figures 1A and 3A). However, during examination of GFP-expressing *H. volcanii* H1206(pJAM1020) biofilm cells, we observed large cellular structures composed of long rods in chains sometimes approaching 30 μm in length (Figure 3B,C,D). These structures were attached to the surface and were found within developing H1206(pJAM1020) biofilms at all observed time points (Figure 3B,C,D; Additional file 2: Movie 1), in several independently transformed H1206(pJAM1020) strains, as well as in biofilms formed by *H. volcanii* strains that do not have the GFP expression plasmid (H53 and H98; see Additional file 1: Figure S2).

Further experimentation verified the relationship between the chained long rod morphotype and biofilm formation in the H1206(pJAM1020) strain. A culture of planktonic cells with an average length of 1.6 μm underwent a morphological shift during the first 12 h of biofilm formation in replicate chamber slide wells (Figure 3E). The difference in length between populations of 2,000 planktonic and 2,000 biofilm cells was statistically significant ($P < 0.0001$ in unpaired *t* test). Cellular structures within biofilms were on average greater than twice as long, were more variable in size (with a standard deviation in length of 3.1 μm) and reached a maximum length ten times greater than that measured within the planktonic culture from which the biofilm was derived (Figure 3E).

***Haloferax volcanii* exhibits social motility following disruption of static liquid biofilms**

An investigation of biofilm dynamics in static liquid began by disrupting mature 7-day biofilms through mechanical homogenization followed by time-lapse photography over a reformation period. To our surprise, this led to the discovery of rapid cellular re-aggregation and sustained coordinated social motility (Figure 4; see Additional files 3, 4, 5, 6 and 7: Movies 2–6). Structured cellular aggregates were visible 3 h following homogenization, after which cell density was incrementally concentrated within a central developing SL-biofilm, with the surrounding medium becoming visibly transparent after 48 h (Figure 4A). Samples were collected from the homogenized biofilm at time zero, and from the central biofilm and surrounding medium at 48 h. The homogenized biofilm was composed of single cells and cellular aggregates; after 48 h, the surrounding medium contained few planktonic cells and the SL-biofilm contained a high density of cells in large aggregates. Images collected during reformation at intervals of 3 h (Figure 4A), 10 min (Figure 4B) and 1 min (see Additional files 3 and 4: Movies 2 and 3) captured the coordination of large filaments of cells into dynamic web-like branches. Rippling or wave-like streaming was observed during extension and retraction of these structures, particularly evident at low frame rates (e.g., see Additional file 4: Movie 3).

Social motility was also triggered by physical agitation or partial disruption of previously undisturbed developing SL-biofilms (see Additional files 5, 6 and 7: Movies 4, 5 and 6). Ring-shaped SL-biofilms, which developed 3 days after an exponential phase culture was left to incubate in replicate Petri dishes under static conditions, formed extensions and migrated towards the perimeter of the dish through a network of apparent cellular streams for over 1.5 h after the culture vessel was gently moved (see Additional file 5: Movie 4). Additional SL-biofilms from the same replicate set retained this sensitivity through day 5 of incubation. As SL-biofilms became denser and reached a stationary phase of growth after 10 days of incubation, identical applications of physical agitation or partial disruption no longer induced social motility. Coordinated motility as shown in Figure 4 and in Movies 2 to 6 (Additional files 3, 4, 5, 6 and 7) has been observed in many independent experiments and is absent in identically prepared heat-treated SL-biofilms (Figure 4A; Additional file 6: Movie 5) and SL-biofilms chemically fixed with formaldehyde (Figure 4A; Additional file 7: Movie 6).

Genetic transfer occurs at high frequency within *Haloferax volcanii* biofilms

A screen for gene transfer within *H. volcanii* biofilms through the known mating mechanism was conducted by cultivating biofilms composed of two strains, each with a

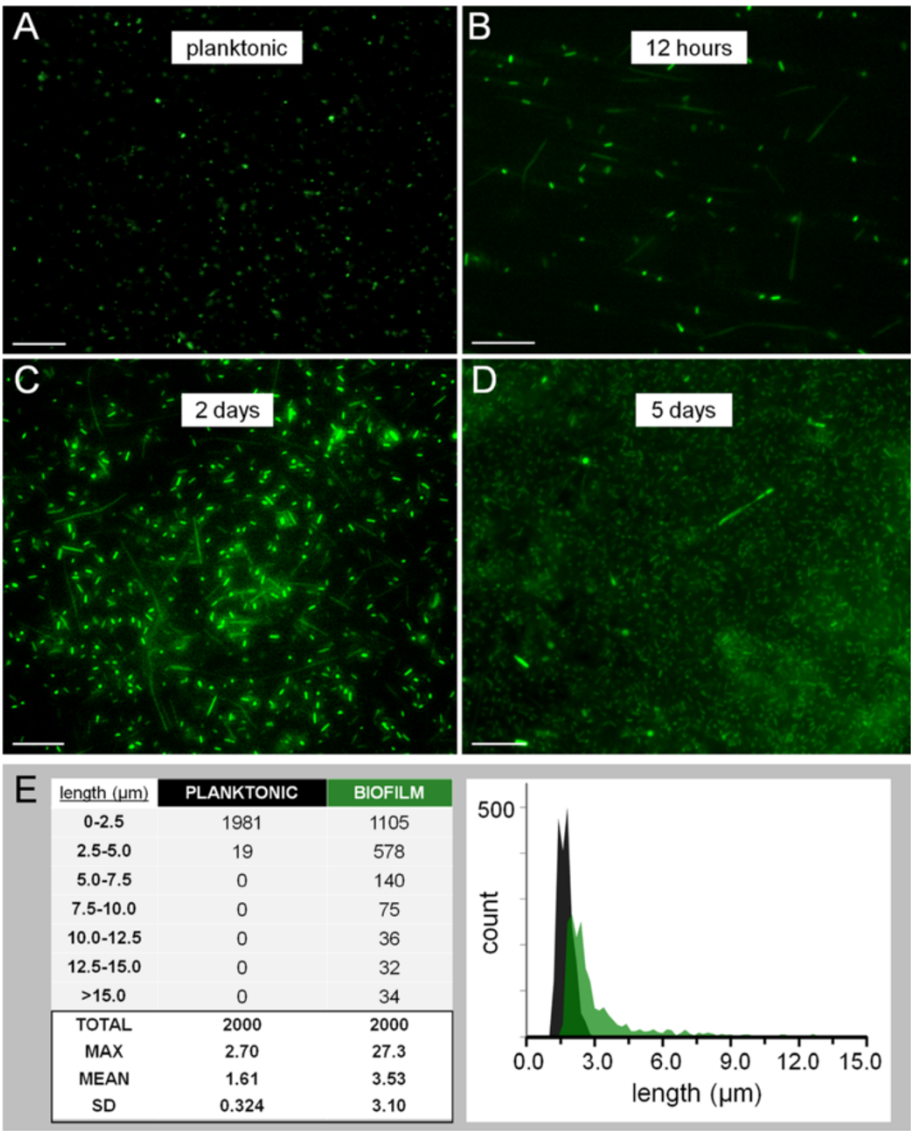


Figure 3 Cellular morphology within developing *Haloferax volcanii* H1206(pJAM1020) static liquid biofilms. (A) Planktonic *H. volcanii* H1206(pJAM1020) cells from exponential phase shaking Hv-YPC culture. (B,C,D) Cells within a developing H1206(pJAM1020) SL-biofilm grown in a chamber slide (in Hv-YPC medium) after 12 h (B), 2 days (C) and 5 days (D). (E) Table listing the number of cells binning into 2.5-μm categories and summarized statistics for 2,000 cells measured for planktonic and biofilm cell populations (left) and histogram showing distribution of length at 0.2-μm binning intervals for planktonic (black) and biofilm (green) cells (right). Cell length was measured with Fiji particle analysis using images collected from three independent exponential phase shaking cultures and three 12 h biofilms grown in chamber slides. Mean length of populations was statistically different with $P < 0.0001$. Scale bars equal 20 μm. SD, standard deviation; SL-biofilm, static liquid biofilm.

unique auxotrophic marker. Gene transfer frequency of the auxotrophic markers was calculated as the number of colonies forming on selective medium (auxotrophs that had regained prototrophy), divided by the number of total viable cells recovered for each culture condition, as described previously [56,57]. A comparison of transfer frequency was conducted for mixed shaking cultures, colony biofilms and SL-biofilms in chamber slides.

Transfer frequencies indicated that the mating mechanism was active within colony biofilms and SL-biofilms

(Figure 5). For chamber slide SL-biofilms, an average transfer frequency of 2.90×10^{-6} was measured and is within the range reported in Mevarech and Werczberger's 1985 study in which mating was first discovered through co-filtering cells on nitrocellulose filters [56]. The transfer frequency for a shaking culture control was low as expected, and mating was not quantifiable in uni-culture biofilms of either H53 or H98 cells (as there is no available source for transfer of the gene required for growth on the selective medium).

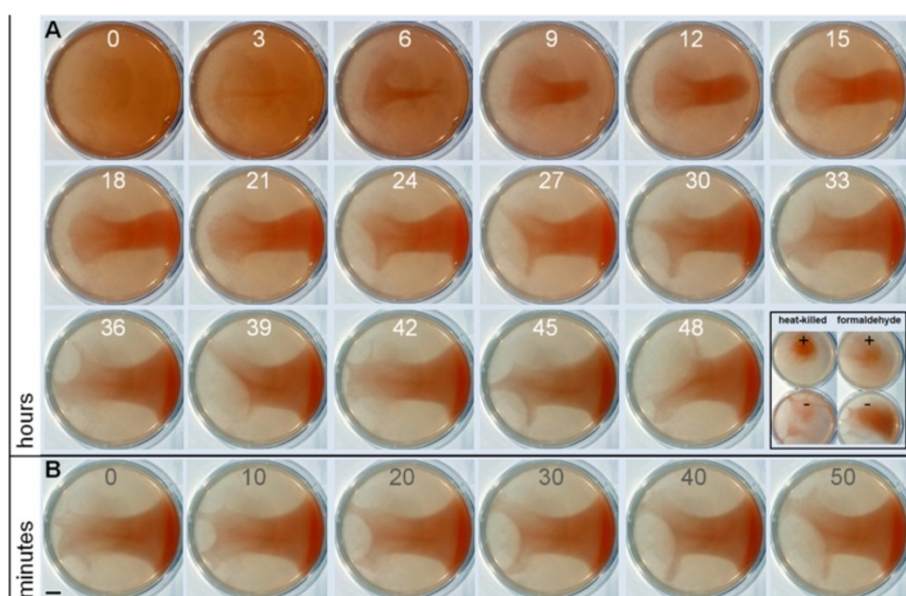


Figure 4 Time-lapse macroscopic photography of static liquid biofilm reformation. An established 7-day SL-biofilm grown in a plastic Petri dish in rich medium (Hv-YPC) was mechanically homogenized and left to incubate at 42°C while photographs were taken at regular time intervals. **(A)** Biofilm reformation over a 2-day period, with images shown at 3 h intervals. Inlay: Cellular vitality controls shown as still images from time-lapse series (see Additional files 6 and 7: Movies 5 and 6) of a SL-biofilm treated with heat (left) and with 4% formaldehyde (right). **(B)** SL-biofilm imaged at 10-min intervals over a 50-min period (a series from between 45 h and 48 h above). Scale bar equals 1 cm. SL-biofilm, static liquid biofilm.

Planktonic (shaking) and SL-biofilm cells were visualized through microscopy in parallel prior to plating to determine whether the cellular morphology was consistent with known models for mating, i.e., that it requires cell-to-cell contact and involves the formation of cytosolic bridges and/or cellular fusion events [58]. Cells from a shaken culture were small and disk-shaped while those in chamber slide biofilms had formed a densely packed basal layer of morphologically diverse cellular structures in close physical association (Additional file 1: Figure S2). Natural transformation has not been reported in *H. volcanii*. In fact, an increase in transfer frequency was reported after adding DNase during mating experiments on filters, indicating that gene transfer in *H. volcanii* biofilms does not occur through transformation [56].

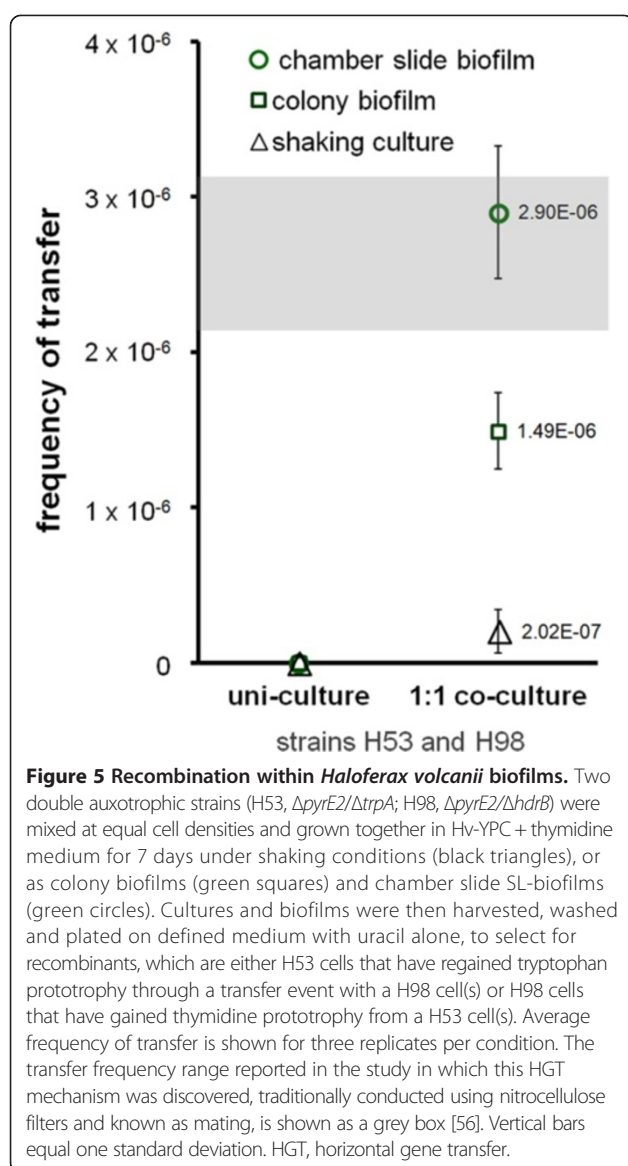
Discussion

Structural development of *Haloferax volcanii* biofilms and biopolymers of the extracellular matrix

The present study and that of Fröls and coworkers [38] demonstrate a propensity of haloarchaeal species to form biofilms and indicate this may be a predominant natural mode of growth for this group of organisms. While haloarchaea are considered extremophiles, the ability of any microbial group to form biofilms is consistent with the emerging view that biofilm formation is an adaptation common to most if not all species [16–19]. In this particular case, the benefits associated with a community lifestyle match the environmental conditions that

challenge microbial life in hypersaline environments. For example, encapsulation within a hydrated nutrient-dense ECM and a biofilm structure with areas that surround developed microcolonies (Figure 1E–H), which likely act as channels to facilitate waste and nutrient exchange, may help explain the persistence of haloarchaeal populations through prolonged periods of starvation [73]. Overall, the delicate and motile nature of multicellular structures imaged in static liquid (Figure 1C–I and Figure 4) may reflect low levels of natural circulation and water activity within hypersaline environments and a selective advantage associated with movement towards favorable conditions.

Our staining experiments with *H. volcanii* H1206 (pJAM1020) allowed for accurate discrimination between cellular structures emitting endogenous GFP signal and ECM and support previous evidence showing that polysaccharide and eDNA are major biofilm components (Figure 2B–E) [38]. Species of the genus *Haloferax* have long been known to produce exopolysaccharide [74] and recent studies of *H. mediterranei* (average nucleotide identity of 86.6% with *H. volcanii* [57]) have identified genes essential for exopolysaccharide synthesis and export [75]. Homologs of genes within an *H. mediterranei* operon shown to be required for exopolysaccharide production [75] are present in the *H. volcanii* genome. Several putative EPS operons have been identified: HVO_2056–HVO_2057 on the main chromosome, and HVO_A0216–A0221 and HVO_A0594–0595 on the mini-



chromosome pHV4. While the function(s) of extracellular DNA within *H. volcanii* ECM is not yet clear, in bacterial biofilms, eDNA is known to be involved in attachment to surfaces, microcolony formation, overall structural integrity and even spatial self-organization [13,76–78]. In several crenarchaeal species, eDNA is present within biofilms but is not a structural component [32]. Similar attempts at DNase treatment of eDNA in haloarchaeal biofilms were unsuccessful and may have been complicated by high salt concentrations within the growth medium [38]. Interestingly, ECM is also known to be a mechanism for nutrient storage [5], and we have previously demonstrated that *H. volcanii* is capable of utilizing eDNA as a nutrient [79,80], suggesting that eDNA may contribute towards the growth of cells within the biofilm.

Bacterial appendages involved in attachment and biofilm formation are often composed of amyloid proteins [27,64,81,82]. Previous studies have surveyed the presence of amyloid in natural biofilms using the dyes CR and ThT and found that it is an abundant and widely distributed ECM component [66,67]. Those same studies reported that amyloid production by archaea could not be determined due to low recovery of archaeal cells from sample sites [66]. On the basis of visible staining with CR, CRF and ThT fluorescence, we have identified putative amyloid protein that was colocalized with *H. volcanii* microcolonies (Figure 2F-M). Although it is most commonly used to stain amyloid fibrils, it is important to note that CR may stain other biopolymers such as polysaccharide [83]. However, because it was colocalized with microcolonies and larger biofilm structures (i.e., not individual cells), CR likely stained a major ECM component and not an internally stored polymer. The gene HVO_1403 is homologous to a known amyloidogenic factor in *Sulfolobus solfataricus* [84] and is a potential genetic determinant of amyloid protein within *H. volcanii* biofilms.

Social motility of static liquid biofilms formed by *Haloferax volcanii* as a multicellular or collective behavior

Macroscopic time-lapse images collected following disruption of SL-biofilms (Figure 4A) demonstrate a propensity for *H. volcanii* cells to re-aggregate within hours, rather than remaining suspended in liquid culture or evenly precipitating. During and after reformation, multicellular filaments or extensions formed, appearing to self-organize and explore the surface area along the bottom of the culture plate (see Additional files 3, 4, 5, 6 and 7: Movies 2–6). This activity was not seen in identically prepared SL-biofilms that had been heat-treated or treated with formaldehyde (see Additional files 6 and 7: Movies 5 and 6, respectively), indicating it is an active biological process, and suggesting the existence of an archaeal system evocative of the elaborate swarming behavior characterized in the soil bacterium *Myxococcus xanthus* [11,85,86] and in *Pseudomonas aeruginosa* [13]. Although swarming is strictly defined as migration across a solid surface [87] and is typically imaged in these species at a solid–air interface, early studies of rippling and wave-formation in *M. xanthus* swarms were also conducted in submerged liquid culture [88,89].

The existence of a system for social motility in *H. volcanii* is supported by the known production of type IV pili-like structures responsible for surface adhesion [90], the prior observation of a hypermotile phenotype [91] and the presence of a complete set of chemotaxis genes (including CheA, CheB, CheC, CheD, CheR and CheW) positioned adjacent and interspersed with archaeal flagella gene clusters (i.e., *flgA1* and *flgA2*) [43,90,91]. A predicted operon including four genes on the main chromosome

(HVO_1221 to 1224) is of particular interest as HVO_1222, HVO_1223 and HVO_1224 proteins are homologs of bacterial frizzy aggregation (Frz)/defective in fruiting (Dif) proteins FrzF, FrzE/DifE and FrzG, respectively, factors that are essential determinants of social motility and ECM production in *M. xanthus* [92]. The ecological role of social motility in *H. volcanii* is undetermined at this point. It is plausible that multicellular groups might migrate towards a nutrient influx during known bloom events [93], or that social motility is associated with an additional activity, such as cooperative feeding.

***Haloferax volcanii* biofilms are hotspots for gene transfer**

While *H. volcanii* is often noted for its unique gene transfer system [56], the mechanism and genes underpinning this phenomenon remain largely uncharacterized [57,94]. Here we report that mating occurs within biofilms at the same frequency as in earlier reports (Figure 5), consistent with the known cell-contact-dependent nature of the mechanism. Mating was discovered and has been routinely observed in the laboratory by several groups by co-precipitating cells or co-filtering them on nitrocellulose filters [56–58,94,95]. These experimental methods for bringing cells together in close proximity can be thought of as proxies for naturally formed biofilms.

We show that *H. volcanii* biofilms contain a biologically formed layer of pleomorphic adherent cells at high density and in close association (Figure 3B,C,D and Additional file 1: Figure S2). The observed spatial arrangement and diversity of cellular structure is consistent with the model of cytoplasmic bridge formation and membrane fusion during mating [95], previous electron micrographs showing elongated cells with intercellular structures [39], and/or the involvement of additional contact-dependent cargo-transfer mechanisms not described in *H. volcanii*, such as lipoprotein transfer [96], vesicular trafficking [97] and cell-to-cell secretion systems [98]. Based on these observations, we suggest biofilms are the microenvironments where mating likely occurs in nature, and propose this mode of growth as an excellent way for studying and visualizing HGT mechanisms in live cells and in real time.

Cellular morphogenesis as phenotypic reflection of differentiation into distinct genetic cell types

In *Bacillus subtilis*, a distinct chained-rod morphology is associated with a population of cells known to produce ECM and to remain attached to the surface, while short unchained rods express flagellar components and are motile [99]. Here, we identified a population of surface-attached cellular structures appearing during biofilm formation and present within developing biofilms but never in planktonic culture (Figure 3; see also Additional file 1: Figure S2 and Additional file 2: Movie 1). Long rod

structures were confirmed as live cells, as the only source of fluorescent signal in Figure 3B,C,D was endogenous GFP. This morphotype is unlikely to be the result of a spontaneous mutation in the H1206(pJAM1020) strain; it was observed in several independent strains and *Haloferax* species are known to have a low spontaneous mutation rate [100].

Our observations are consistent with reports of “irregular” morphological characteristics (labeled as “involution forms” or “hyphomicrobium-like” structures) when *H. volcanii* DS2 is grown on agar medium, as noted in the original 1975 characterization [39]. Archaeosortase (*artA*) overexpression strains also showed an elongated rod morphology. The ArtA protein has many downstream targets effecting cell shape and surface decoration, indicating that it could be a regulatory component of biofilm formation and/or related systems [94]. Previous observations of irregular cell morphologies can now be understood as being coupled with biofilm formation.

Additional cellular functions may also be associated with a chained-rod or adherent cell phenotype. Larsen and Mullakhanbhai [39] found narrow constrictions with an apparently contiguous S-layer connecting cells together like beads on a string. In light of the later discovery of the mating HGT mechanism and electron micrographs of mating cells, the constrictions and associations between GFP-expressing cells observed in biofilms in this study (Figure 3B,C,D; Additional file 1: Figure S2 and Additional file 2: Movie 1) may be viewed as cytoplasmic bridges, which have been proposed as a prerequisite step towards cellular fusion and chromosomal mixing and/or recombination [56–58,95]. Further genetic analyses will shed light on the possible specialized function(s) (e.g., matrix-production or competence for mating) of this cellular phenotype.

Conclusions

The archaeon *H. volcanii* forms biofilms in several experimental systems that can be visualized in the laboratory using standard protocols developed for bacterial species. *H. volcanii* cells develop into biofilm structures that exhibit complexity in both cellular morphology and ECM composition. We have reported several key features of *H. volcanii* biofilms: structural development through microcolony formation and maturation phases, visualization of ECM, including the identification of putative amyloid fibrils, an archaeal form of social motility, as well as a chained-long rod morphotype and gene transfer. With the implementation of fluorescent proteins for biofilm visualization and the available genetic system, it is clear that the study of biofilm formation in *H. volcanii* is not only a means for understanding haloarchaeal ecology and physiology, but also acts as an excellent model for the molecular biology of archaeal biofilms and multicellular

behaviors. Future studies may focus on the genetic identification of many possible differentiated cell types and the visualization of their positions in time and space using fluorescent protein reporters. The likely many genetic determinants of ECM components, social motility and the enigmatic mating mechanism for gene transfer in *H. volcanii* all remain to be discovered.

Methods

Strains and culture media

H. volcanii strains (see Additional file 1: Table S2) were provided by Thorsten Allers of the University of Nottingham, UK, and grown in media adapted from previous studies [47]. Rich medium (Hv-YPC) contained 144 g NaCl, 21 g $\text{MgSO}_4 \times 7\text{H}_2\text{O}$, 18 g $\text{MgCl}_2 \times 6\text{H}_2\text{O}$, 4.2 g KCl, 12 mM Tris-HCl pH 7.5, 3.125 ml 1 M CaCl_2 solution, 1.0 ml trace element solution, 5.0 g yeast extract, 1.0 g casamino acids, and 1.0 g peptone per liter. Hv-YPC used to culture GFP biofilms for EPS staining also contained 0.5% glucose.

Hv-Ca medium contained 144 g NaCl, 21 g $\text{MgSO}_4 \times 7\text{H}_2\text{O}$, 18 g $\text{MgCl}_2 \times 6\text{H}_2\text{O}$, 4.2 g KCl, 12 mM Tris-HCl pH 7.5, 3.125 ml 1 M CaCl_2 solution, 1.0 ml trace element solution, 5.0 g casamino acids, 0.125 ml 6.4 mg/ml thiamine solution, and 0.125 ml 0.8 mg/ml biotin solution per liter.

A basal-salts starvation medium (Hv-starve) contained all components in Hv-YPC other than complex nutrients (i.e., yeast extract, casamino acids and peptone). Solid media contained 18 g of agar per liter. When required, uracil was provided at 50 $\mu\text{g}/\text{ml}$ (ΔpyrE2 strains), thymidine and hypoxanthine at 40 $\mu\text{g}/\text{ml}$ (ΔhdrB strains), tryptophan at 50 $\mu\text{g}/\text{ml}$ (ΔtrpA strains), and novobiocin at 0.30 $\mu\text{g}/\text{ml}$ for antibiotic selection.

Development of GFP-expressing *Haloferax volcanii* H1206 strain

Two *H. volcanii* uracil auxotrophic strains were developed for constitutive GFP-expression and cell imaging by CLSM and epifluorescence microscopy (see Additional file 1: Table S2). The strain H1206(pJAM1020) was based on selection through novobiocin resistance using a previously developed vector [59], and a second strain H1206 (pSC409GFP) was based on the gene *pyrE2* and uracil autotrophy [44,46,47]. Plasmid pSC409GFP was constructed by amplifying the region from pJAM1020 containing red-shifted GFP and P2 promoter for constitutive expression in haloarchaeal species [59], and inserting this construct into the shuttle vector pTA409 [101] (see Additional file 1: Tables S2 and S3). Each plasmid was transformed into the strain H1206 (ΔpyrE2 Δmrr) using the PEG-based method as previously developed [49,102,103], and transformants were selected on Hv-Ca medium without uracil for H1206(pSC409GFP) or

containing novobiocin for H1206(pJAM1020). *H. volcanii* H1206 is identical to H26 other than an additional deletion of the *mrr* gene, which encodes a restriction endonuclease that cleaves methylated foreign DNA, allowing transformation without passage through an *Escherichia coli* *dam* mutant [46]. Growth kinetics of each GFP strain in liquid Hv-YPC medium were measured by optical density and were unchanged from the parental strain.

Biofilm growth systems

The media described above were prepared and used to cultivate *H. volcanii* biofilms using the experimental growth methods described below. All biofilms were incubated at 42°C unless otherwise stated.

Colony biofilms

Colony biofilms as shown in Figure 1B were prepared on 13-mm polycarbonate filters (0.2- μm pore size, Sigma, St. Louis, MO, Z365041) as previously described [7,23]. Diluted *H. volcanii* culture ($\text{OD}_{600\text{ nm}} = 0.1$) was transferred onto the surface of sterile filters previously placed directly on the surface of the solid medium with sterile forceps. After the culture medium penetrated the filter and evaporated, the plates were inverted and incubated. Filters were transferred to fresh plates under sterile conditions every 48 h during the growth period.

Static liquid biofilms

SL-biofilms were set up by aliquoting inoculated growth medium into six-well plates and Petri dishes (as in Figures 1C, 2K and 4, and see Additional files 3, 4, 5, 6 and 7: Movies 2–6), or chamber slides (Lab-Tek II, with 0.7 cm^2 growth area per well; as in the top left panel of Figure 1C and Figure 2I,J). A borosilicate glass coupon (Biosurfaces Technologies Corporation, Bozeman, MT, RD 128-GL) or a piece of coverglass was placed inside the six-well plates (as in Figure 1C) to provide a biofilm growth surface that could be visualized directly through microscopy.

Biofilm staining and microscopy preparation

The properties and experimental parameters used for all dyes in this study are summarized in Additional file 1: Table S1. The final concentration of each staining solution was optimized based on either the manufacturer's protocol or a previous study. CR staining was performed using the alkaline CR method [104,105]. Biofilms were stained and prepared for microscopy as described below for each growth method.

Colony biofilms

Mature colony biofilms were stained by transferring a staining solution in Hv-starve medium directly on top of the colony biofilm and incubating at room temperature for 60 min. Cross sections of stained colony biofilms

(e.g., Figure 1B) were cryo-processed by rapid freezing on dry ice and cross-sectioned using a Leica CM1850 cryostat microtome as described previously [23]. Then, the 5- μ m transects were placed onto microscope slides and visualized immediately.

Glass surfaces within SL-biofilms

Staining on glass coupons and coverglass was conducted by removing the growth substrate from the growth system/medium, followed by placement in fresh sterile 60-mm Petri dishes. An Hv-starve staining solution was then gently transferred (immediately, before the remaining culture medium on the surface of the glass evaporated) to the surface of the substrate (i.e. glass coupon), completely covering the surface. This volume of staining solution remained on the surface through surface tension during a 60-min staining period at room temperature in the dark. The staining solution was then carefully removed and the surface was washed once with Hv-starve (same volume as used for staining solution). The substrate was then placed in a new Petri dish and fresh Hv-starve medium was added until the surface of the growth surface was submerged by approximately 5 mm.

Chamber slides

Biofilms grown in chamber slides were stained by removing conditioned medium from the wells through gentle aspiration, followed by the addition of Hv-starve staining solution (same volume as medium used to grow biofilm, e.g. 500 μ l) for 60 min at room temperature in the dark. Staining solution was then removed, the surface was gently washed once with the addition and subsequent removal of another equal volume of Hv-starve, and fresh Hv-starve was added, followed by direct visualization.

Fluorescence microscopy and imaging

Confocal microscopy

An upright Leica Microsystems (Wetzlar, Germany) TCS SP5 laser-scanning confocal microscope was used (for data shown in Figure 1D-I) with a 63 \times water immersion lens placed directly into the bulk fluid above biofilms grown on glass coupons or coverglass. Images were acquired through the Leica Application Suite Advanced Fluorescence software platform. Three-dimensional reconstructions of focal plane slices were generated and analyzed using IMARIS from Bitplane (Zürich, Switzerland; Figure 1D-H) or Fiji [106]. An Andor spinning disk confocal system with a Nikon Eclipse Ti microscope (data shown in Figure 2C,D,E,M) and Nikon A1R Spectral Confocal Microscope (Additional file 1: Figure S2) were also used to image live biofilms within chamber slides.

Two-dimensional microscopy

Images were collected using an upright Nikon Eclipse E800 epifluorescent microscope, also with water immersion

lenses placed directly above cultured biofilms. For biofilms grown in chamber slides, they were collected with an inverted Nikon Eclipse TE300 with a SPOT digital microscope camera (shown in Figures 1A,B, 2B, F-H and 3A-D, and Additional file 1: Figures S1,S2,S3 and Additional file 2: Movie 1).

Macroscopic imaging

Colonies and SL-biofilms in chamber slides were imaged using a Zeiss Discovery V20 stereo fluorescence dissecting microscope with a Zeiss AxioCam camera (Figures 1C and 2A,I-L and Additional file 1: Figure S1). Photographs of live SL-biofilms in time-lapse studies were taken using a digital single-lens reflex camera and macro lens, LED light source and intervalometer mounted within an incubator (Figure 4 and Additional files 3, 4, 5, 6 and 7: Movies 2–6).

Additional imaging details

No autofluorescence signals were detected from *H. volcanii* cells or biofilm structures in all excitation channels used in this study (for excitation wavelengths used for each dye, see Additional file 1: Table S1). Images collected with black and white digital cameras were pseudo-colored with the respective observed fluorescent emission signal.

Measurement of cellular morphology and biofilm structure

Cell lengths and dimensions of biofilm structures were measured using Fiji as developed by the National Institutes of Health [106]. Analysis of cell length for planktonic and biofilm cell populations in Figure 3E included 2,000 cells each from three separate images collected from three independent replicates under identical conditions. Mid-exponential phase ($OD_{600\text{ nm}} = 0.4$ to 0.5) replicate planktonic cultures of strain H1206(pJAM1020) were imaged, diluted (to $OD_{600\text{ nm}} = 0.1$) in fresh medium (Hv-YPG +0.5% glucose), and 500 μ l aliquots were transferred to replicate chamber-slide wells. Measurements were generated using the analyze particles function of Fiji [106].

Preparation for macroscopic time-lapse studies and induction of social motility

Disruption and reformation

SL-biofilms shown in Figure 4, Additional file 3: Movie 2 and Additional file 4: Movie 3 were established by transferring the liquid culture ($OD_{600\text{ nm}} = 1.0$) into Petri dishes and incubating under static conditions for 7 days. These mature SL-biofilms were then mechanically homogenized through repetitive pipetting with a serological pipette to disrupt the layer of attached biofilm and large loosely attached aggregates. This was followed by transfer into a conical tube and gentle vortexing. The homogenized SL-biofilm culture was then transferred back into the original culture dish and left to incubate while photographs were collected.

Physical agitation

The SL-biofilm in Additional file 5: Movie 4 had formed after a liquid culture of *H. volcanii* H53 cells that had been freshly diluted in Hv-YPC medium (to OD_{600 nm} = 0.25) was transferred to Petri dishes and left to incubate for 5 days. Social motility as accessed by rapid formation of cellular extensions was induced in these biofilms by tapping the lid of the Petri dish, or by gently lifting and re-lowering the Petri dish approximately 1 cm. Such agitation did not disturb the overall biofilm; however, it caused smaller defects in loose biofilm structures, which were followed by prolonged social motility.

Control treatments

Established 7-day SL-biofilms were heat-treated within the culture dish at 75°C for 1 h or left untreated, but prepared for time-lapse observation identically (i.e., moved the same distance and partially disrupted during handling). Samples removed from heat-treated and untreated biofilms, stained with propidium iodide and prepared on microscope slides, verified that heat treatment left cells dead but intact, appearing like spheroplasts. Cells within SL-biofilms were also fixed by adding 37% formaldehyde (Fisher Chemical, Waltham, MA, F79-500) to a final concentration of 4% and incubating for 1 h prior to imaging as an additional control for cellular vitality.

Biofilm recombination assay

Recombination within *H. volcanii* SL-biofilms was quantified using an approach adapted from a previously described method whereby two double auxotrophic strains are mixed and passed into nitrocellulose filters [56–58]. The strain H53, a uracil and tryptophan auxotroph, and the strain H98, a uracil and thymidine auxotroph (see Additional file 1: Table S2), where grown to late exponential phase (OD_{600 nm} 0.60 to 0.80) in Hv-YPC + thy, diluted (to OD_{600 nm} = 0.50), mixed together in equal parts and transferred into chamber slides or on top of filters for colony biofilm development.

SL-biofilms and colony biofilms were incubated and allowed to grow for 7 days, during which a biofilm developed (see Additional file 1: Figure S2). Static biofilms were then harvested by mechanical disruption through repetitive pipetting to detach the biofilm, followed by vortexing within a conical tube. Colony biofilms were placed into 1.5-ml tubes with 1 ml of Hv-starve medium with sterile forceps, vortexed and then shaken at 180 rpm for 1 h at 42°C to release cells for plating. An identical mixture of H53 and H98 liquid culture was also left shaking at 180 rpm for 7 days as a negative control. Samples for each condition were washed three times with Hv-starve medium, resuspended in Hv-starve and plated on Hv-Ca with uracil as selective screen for H53 and H98 prototrophic revertants and Hv-YPC + thy for total viable counts. Pure cultures

of H53 and H98 were included for each condition as a negative control for mating. Plating on Hv-Ca medium without uracil was also included in the experiment to control for spontaneous reversion to uracil prototrophy (although this was not likely as the *pyrE2* gene is not mutated in H53/H98, but is completely deleted) or the presence of any ura⁺ strain; no colonies were observed for any of these conditions. The transfer frequency was calculated by dividing the average number of colony-forming units (CFU) per ml on selective medium (Hv-Ca with uracil) for each replicate set by the corresponding averaged total CFU count (CFU/ml on Hv-YPC + thy medium).

Additional files

Additional file 1: The file contains Figures S1 to S3 and Tables S1 to S3. Figure S1. Colonies formed by *Haloferax volcanii* H1206(pSC409GFP). **Figure S2.** The basal layer of a 7-day H53/H98 mixed SL-biofilm stained with SYTO 9 at the time cells were plated for the recombination experiment shown in Figure 5. **Figure S3.** Seven-day *H. volcanii* H1206(pJAM1020) SL-biofilm stained with Congo red. **Table S1.** Cellular/matrix stains and fluorescent proteins used for biofilm visualization. **Table S2.** Strains and plasmids. **Table S3.** Oligonucleotide primers.

Additional file 2: Movie 1. Time-lapse microscopy of long rods/adherent cellular structures within a developing 12-h *Haloferax volcanii* H1206 (pJAM1020) SL-biofilm under blue excitation. Images were collected at 2-s intervals and replayed at 4 frames per second (8x real time).

Additional file 3: Movie 2. Macroscopic time-lapse microscopy of a 7-day *Haloferax volcanii* H53 SL-biofilm following disruption and reformation. Fifteen hours of images are shown, collected after images shown in Figure 4, at 1-min intervals and replayed at 14 frames per second (840x real time).

Additional file 4: Movie 3. Motility in wave-like patterns observed during macroscopic time-lapse photography of a 7-day *Haloferax volcanii* H53 SL-biofilm following disruption and reformation. Thirty minutes of images are shown (a subset of the data series in Movie 2) at 1-min intervals and replayed at 3 frames per second (180x real time).

Additional file 5: Movie 4. Macroscopic time-lapse microscopy of a 5-day *Haloferax volcanii* H53 SL-biofilm. Ninety minutes of images are shown immediately following physical agitation without complete disruption of the biofilm at 10-s intervals and replayed at 30 frames per second (300x real time).

Additional file 6: Movie 5. Macroscopic time-lapse microscopy of heat-treated (A) and untreated (B) 7-day *Haloferax volcanii* H53 SL-biofilms. Three hours of images are shown, collected at 30-s intervals and replayed at 14 frames per second (420x real time).

Additional file 7: Movie 6. Macroscopic time-lapse microscopy of 7-day *Haloferax volcanii* H53 SL-biofilms treated with 4% formaldehyde (A) or left untreated (B). Eighty minutes of images are shown, collected at 30-s intervals and replayed at 14 frames per second (420x real time).

Abbreviations

CLSM: confocal laser scanning microscopy; ConA: concanavalin A; CMO: CellMask Orange; CR: Congo red; CRF: Congo red fluorescence; DAPI: 4',6-diamidino-2-phenylindole; DDAO: 7-hydroxy-9H-1-3-dichloro-9,9-dimethylacridin-2-one; ECM: extracellular matrix; eDNA: extracellular DNA; EPS: extracellular polymeric substance; GFP: green fluorescent protein; HGT: horizontal gene transfer; PEG: poly(ethylene) glycol; SL-biofilm: static liquid biofilm; ThT: thioflavin T.

Competing interests

The authors declare that the research was conducted in the absence of any commercial or financial relationships that could be construed as a potential conflict of interest.

Authors' contributions

SC, MF and RTP conceived of the research and designed the experiments. SC carried out the experiments, and SC, MF and RTP analyzed the experiments and wrote the manuscript. All authors have read and approved the final manuscript.

Acknowledgements

We thank the Center for Biofilm Engineering (CBE) at Montana State University, Bozeman. We are especially grateful to Betsey Pitts and Kerry Williamson from the CBE for microscopy guidance and assistance, and to Thorsten Allers and Julie Maupin-Furlow for the *Haloferax* strains and plasmids. This research was supported by the National Science Foundation (award numbers DEB0919290 and DEB0830024) and NASA Astrobiology: Exobiology and Evolutionary Biology Program Element (grant number NNX12AD70G).

Author details

¹Department of Molecular and Cell Biology, University of Connecticut, Storrs, Connecticut, USA. ²Department of Microbiology and Center for Biofilm Engineering, Montana State University, Bozeman, MT, USA.

Received: 6 May 2014 Accepted: 31 July 2014

Published online: 14 August 2014

References

- Aguilar C, Vlamakis H, Losick R, Kolter R: **Thinking about *Bacillus subtilis* as a multicellular organism.** *Curr Opin Microbiol* 2007, **10**:638–643.
- Watnick P, Kolter R: **Biofilm, city of microbes.** *J Bacteriol* 2000, **182**:2675–2679.
- Parsek MR, Greenberg EP: **Sociomicrobiology: the connections between quorum sensing and biofilms.** *Trends Microbiol* 2005, **13**:27–33.
- Branda SS, Vik S, Friedman L, Kolter R: **Biofilms: the matrix revisited.** *Trends Microbiol* 2005, **13**:20–26.
- Flemming HC, Wingender J: **The biofilm matrix.** *Nat Rev Microbiol* 2010, **8**:623–633.
- Matz C, Webb JS, Schupp PJ, Phang SY, Penesyan A, Egan S, Steinberg E, Kjelleberg S: **Marine biofilm bacteria evade eukaryotic predation by targeted chemical defense.** *PLoS One* 2008, **3**:e2744.
- Anderl JN, Franklin MJ, Stewart PS: **Role of antibiotic penetration limitation in *Klebsiella pneumoniae* biofilm resistance to ampicillin and ciprofloxacin.** *Antimicrob Agents Chemother* 2000, **44**:1818–1824.
- Chiang WC, Nilsson M, Jensen PO, Hoiby N, Nielsen TE, Givskov M, Tolker-Nielsen T: **Extracellular DNA shields against aminoglycosides in *Pseudomonas aeruginosa* biofilms.** *Antimicrob Agents Chemother* 2013, **57**:2352–2361.
- Molin S, Tolker-Nielsen T: **Gene transfer occurs with enhanced efficiency in biofilms and induces enhanced stabilisation of the biofilm structure.** *Curr Opin Biotechnol* 2003, **14**:255–261.
- Nguyen KT, Pliastro K, Gray TA, Derbyshire KM: **Mycobacterial biofilms facilitate horizontal DNA transfer between strains of *Mycobacterium smegmatis*.** *J Bacteriol* 2010, **192**:5134–5142.
- Li Y, Sun H, Ma X, Lu A, Lux R, Zusman D, Shi W: **Extracellular polysaccharides mediate pilus retraction during social motility of *Myxococcus xanthus*.** *Proc Natl Acad Sci USA* 2003, **100**:5443–5448.
- Welch R, Kaiser D: **Cell behavior in traveling wave patterns of myxobacteria.** *Proc Natl Acad Sci USA* 2001, **98**:14907–14912.
- Gloag ES, Turnbull L, Huang A, Vallotton P, Wang H, Nolan LM, Mililli L, Hunt C, Lu J, Osvath SR, Monahan LG, Cavaliere R, Charles IG, Wand MP, Gee ML, Prabhakar R, Whitchurch CB: **Self-organization of bacterial biofilms is facilitated by extracellular DNA.** *Proc Natl Acad Sci USA* 2013, **110**:11541–11546.
- Shapiro JA: **Bacteria as multicellular organisms.** *Sci Am* 1988, **256**:82–89.
- Claessen D, Rozen DE, Kuipers OP, Sogaard-Andersen L, van Wezel GP: **Bacterial solutions to multicellularity: a tale of biofilms, filaments and fruiting bodies.** *Nat Rev Microbiol* 2014, **12**:115–124.
- Kolter R, Kornberg EP: **The superficial life of microbes.** *Nature* 2006, **441**:300–302.
- Costerton JW, Lewandowski Z: **Microbial biofilms.** *Annu Rev Microbiol* 1995, **49**:711–745.
- Costerton JW, Lewandowski Z, De Beer D, Caldwell D, Korber D, James G: **Biofilms, the customized microniche.** *J Bacteriol* 1994, **176**:2137–2142.
- Davey ME, O'Toole GA: **Microbial biofilms: from ecology to molecular genetics.** *Microbiol Mol Biol Rev* 2000, **64**:847–867.
- Geesey GG, Mutch R, Costerton JW, Green RB: **Sessile bacteria: an important component of the microbial population in small mountain streams.** *Limnol Oceanogr* 1978, **23**:1214–1223.
- O'Toole G, Kaplan HB, Kolter R: **Biofilm formation as microbial development.** *Annu Rev Microbiol* 2000, **57**:49–79.
- Stoodley P, Sauer K, Davies DG, Costerton JW: **Biofilms as complex differentiated communities.** *Annu Rev Microbiol* 2002, **56**:187–209.
- Lenz AP, Williamson KS, Pitts B, Stewart PS, Franklin MJ: **Localized gene expression in *Pseudomonas aeruginosa* biofilms.** *Appl Environ Microbiol* 2008, **74**:4463–4471.
- Vlamakis H, Aguilar C, Losick R, Kolter R: **Control of cell fate by the formation of an architecturally complex bacterial community.** *Genes Dev* 2008, **22**:945–953.
- Stewart PS, Franklin MJ: **Physiological heterogeneity in biofilms.** *Nat Rev Microbiol* 2008, **6**:199–210.
- Lopez D, Vlamakis H, Kolter R: **Generation of multiple cell types in *Bacillus subtilis*.** *FEMS Microbiol Rev* 2009, **33**:152–163.
- Romero D, Aguilar C, Losick R, Kolter R: **Amyloid fibers provide structural integrity to *Bacillus subtilis* biofilms.** *Proc Natl Acad Sci USA* 2010, **107**:2230–2234.
- Flemming HC, Neu TR, Wozniak DJ: **The EPS matrix: the 'house of biofilm cells'.** *J Bacteriol* 2007, **189**:7945–7947.
- Friedman L, Kolter R: **Genes involved in matrix formation in *Pseudomonas aeruginosa* PA14 biofilms.** *Mol Microbiol* 2003, **51**:675–690.
- Orell A, Fröls S, Albers SV: **Archaeal biofilms: the great unexplored.** *Annu Rev Microbiol* 2013, **67**:337–354.
- Fröls S: **Archaeal biofilms: widespread and complex.** *Biochem Soc Trans* 2013, **41**:393–398.
- Koerd A, Godeke J, Berger J, Thormann KM, Albers SV: **Crenarchaeal biofilm formation under extreme conditions.** *PLoS One* 2010, **5**:e14104.
- Orell A, Peeters E, Vassen V, Jachlewski S, Schalles S, Siebers B, Albers SV: **Lrs14 transcriptional regulators influence biofilm formation and cell motility of Crenarchaea.** *ISME J* 2013, **7**:1886–1898.
- Henche AL, Koerd A, Ghosh A, Albers SV: **Influence of cell surface structures on crenarchaeal biofilm formation using a thermostable green fluorescent protein.** *Environ Microbiol* 2012, **14**:779–793.
- Baker-Austin C, Potrykus J, Wexler M, Bond PL, Dopson M: **Biofilm development in the extremely acidophilic archaeon 'Ferroplasma acidimanus' Fer1.** *Extremophiles* 2010, **14**:485–491.
- Henneberger R, Moissl C, Amann T, Rudolph C, Huber R: **New insights into the lifestyle of the cold-loving SM1 euryarchaeon: natural growth as a monospecies biofilm in the subsurface.** *Appl Environ Microbiol* 2006, **72**:192–199.
- Rudolph C, Moissl C, Henneberger R, Huber R: **Ecology and microbial structures of archaeal/bacterial strings-of-pearls communities and archaeal relatives thriving in cold sulfidic springs.** *FEMS Microbiol Ecol* 2004, **50**:1–11.
- Fröls S, Dyall-Smith M, Pfeifer F: **Biofilm formation by haloarchaea.** *Environ Microbiol* 2012, **14**:3159–3174.
- Mullakhanbhai MF, Larsen H: ***Halo bacterium volcanii* spec. nov., a Dead Sea halobacterium with a moderate salt requirement.** *Arch Microbiol* 1975, **104**:207–214.
- Jantzer K, Zerulla K, Soppa J: **Phenotyping in the Archaea: optimization of growth parameters and analysis of mutants of *Haloferax volcanii*.** *FEMS Microbiol Lett* 2011, **322**:123–130.
- Robinson JL, Pyzyra B, Atrasz RG, Henderson CA, Morrill KL, Burd AM, Desoucy E, Fogleman RE 3rd, Naylor JB, Steele SM, Elliott DR, Leyva KJ, Shand RF: **Growth kinetics of extremely halophilic Archaea (family Halobacteriaceae) as revealed by Arrhenius plots.** *J Bacteriol* 2005, **187**:923–929.
- Soppa J: **From genomes to function: haloarchaea as model organisms.** *Microbiology* 2006, **152**:585–590.
- Hartman AL, Norais C, Badger JH, Delmas S, Haldenby S, Madupu R, Robinson J, Khouri H, Ren Q, Lowe TM, Maupin-Furlow J, Pohlschroder M, Daniels C, Pfeiffer F, Allers T, Eisen JA: **The complete genome sequence of *Haloferax volcanii* DS2, a model archaeon.** *PLoS One* 2010, **5**:e9605.
- Allers T, Mevarech M: **Archaeal genetics - the third way.** *Nat Rev Genet* 2005, **6**:58–73.
- Leigh JA, Albers SV, Atomi H, Allers T: **Model organisms for genetics in the domain Archaea: methanogens, halophiles, Thermococcales and Sulfolobales.** *FEMS Microbiol Rev* 2011, **35**:577–608.
- Allers T, Barak S, Liddell S, Wardell K, Mevarech M: **Improved strains and plasmid vectors for conditional overexpression of His-tagged proteins in *Haloferax volcanii*.** *Appl Environ Microbiol* 2010, **76**:1759–1769.
- Allers T, Ngo HP, Mevarech M, Lloyd RG: **Development of additional selectable markers for the halophilic archaeon *Haloferax volcanii* based on the leuB and trpA genes.** *Appl Environ Microbiol* 2004, **70**:943–953.

48. Blaby IK, Phillips G, Blaby-Haas CE, Gulig KS, El Yacoubi B, de Crecy-Lagard V: **Towards a systems approach in the genetic analysis of Archaea: accelerating mutant construction and phenotypic analysis in *Haloferax volcanii*.** *Archaea* 2010, **2010**:426239.
49. Bitan-Banin G, Ortenberg R, Mevarech M: **Development of a gene knockout system for the halophilic archaeon *Haloferax volcanii* by use of the *pyrE* gene.** *J Bacteriol* 2003, **185**:772-778.
50. Papke RT, Koenig JE, Rodriguez-Valera F, Doolittle WF: **Frequent recombination in a saltwater population of *Halorubrum*.** *Science* 2004, **306**:1928-1929.
51. DeMaere MZ, Williams TJ, Allen MA, Brown MV, Gibson JA, Rich J, Lauro FM, Dyall-Smith M, Davenport KW, Woyke T, Kyripides NC, Tringe SG, Cavicchioli R: **High level of intergenera gene exchange shapes the evolution of haloarchaea in an isolated Antarctic lake.** *Proc Natl Acad Sci USA* 2013, **110**:16939-16944.
52. Ram Mohan N, Fullmer MS, Makkay AM, Wheeler R, Ventosa A, Naor A, Gogarten JP, Papke RT: **Evidence from phylogenetic and genome fingerprinting analyses suggests rapidly changing variation in *Halorubrum* and *Haloarcula* populations.** *Front Microbiol* 2014, **5**:143.
53. Papke RT, Zhaxybayeva O, Feil EJ, Sommerfeld K, Muise D, Doolittle WF: **Searching for species in haloarchaea.** *Proc Natl Acad Sci USA* 2007, **104**:14092-14097.
54. Fullmer MS, Soucy SM, Swithers KS, Makkay AM, Wheeler R, Ventosa A, Gogarten JP, Papke RT: **Population and genomic analysis of the genus *Halorubrum*.** *Front Microbiol* 2014, **5**:140.
55. Dillon JG, Carlin M, Gutierrez A, Nguyen V, McLain N: **Patterns of microbial diversity along a salinity gradient in the Guerrero Negro solar saltern, Baja CA Sur, Mexico.** *Front Microbiol* 2013, **4**:399.
56. Mevarech M, Werczberger R: **Genetic transfer in *Halobacterium volcanii*.** *J Bacteriol* 1985, **162**:461.
57. Naor A, Lapiere P, Mevarech M, Papke RT, Gophna U: **Low species barriers in halophilic Archaea and the formation of recombinant hybrids.** *Curr Biol* 2012, **22**:1444-1448.
58. Rosenshine I, Tchelet R, Mevarech M: **The mechanism of DNA transfer in the mating system of an archaeobacterium.** *Science* 1989, **245**:1387-1389.
59. Reuter CJ, Maupin-Furlow JA: **Analysis of proteasome-dependent proteolysis in *Haloferax volcanii* cells, using short-lived green fluorescent proteins.** *Appl Environ Microbiol* 2004, **70**:7530-7538.
60. Marcus A, Sadimin E, Richardson M, Goodell L, Fyfe B: **Fluorescence microscopy is superior to polarized microscopy for detecting amyloid deposits in Congo red-stained trephine bone marrow biopsy specimens.** *Am J Clin Pathol* 2012, **138**:590-593.
61. Hsiao K, Chapman P, Nilsen S, Eckman C, Harigaya Y, Younkin S, Yang F, Cole G: **Correlative memory deficits, A β elevation, and amyloid plaques in transgenic mice.** *Science* 1996, **274**:99-102.
62. Wilcock DM, Gordon MN, Morgan D: **Quantification of cerebral amyloid angiopathy and parenchymal amyloid plaques with Congo red histochemical stain.** *Nat Protoc* 2006, **1**:1591-1595.
63. Puchtler H, Sweat F, Levine M: **On the binding of Congo red by amyloid.** *J Histochem Cytochemistry* 1962, **10**:355-364.
64. Chapman MR, Robinson LS, Pinkner JS, Roth R, Heuser J, Hammar M, Normark S, Hultgren SJ: **Role of *Escherichia coli* curli operons in directing amyloid fiber formation.** *Science* 2002, **295**:851-855.
65. Kaiser TD, Pereira EM, Dos Santos KR, Maciel EL, Schuenck RP, Nunes AP: **Modification of the Congo red agar method to detect biofilm production by *Staphylococcus epidermidis*.** *Diagn Microbiol Infect Dis* 2013, **75**:235-239.
66. Larsen P, Nielsen JL, Dueholm MS, Wetzel R, Otzen D, Nielsen PH: **Amyloid adhesins are abundant in natural biofilms.** *Environ Microbiol* 2007, **9**:3077-3090.
67. Larsen P, Nielsen JL, Otzen D, Nielsen PH: **Amyloid-like adhesins produced by floc-forming and filamentous bacteria in activated sludge.** *Appl Environ Microbiol* 2008, **74**:1517-1526.
68. Romero D, Vlamakis H, Losick R, Kolter R: **An accessory protein required for anchoring and assembly of amyloid fibres in *B. subtilis* biofilms.** *Mol Microbiol* 2011, **80**:1155-1168.
69. Chai L, Romero D, Kayatekin C, Akabayov B, Vlamakis H, Losick R, Kolter R: **Isolation, characterization, and aggregation of a structured bacterial matrix precursor.** *J Biol Chem* 2013, **288**:17559-17568.
70. Jonas K, Tomenius H, Kader A, Normark S, Romling U, Belova LM, Melefors O: **Roles of curli, cellulose and BapA in *Salmonella* biofilm morphology studied by atomic force microscopy.** *BMC Microbiol* 2007, **7**:70.
71. Freeman DJ, Falkner FR, Keane CT: **New method for detecting slime production by coagulase negative staphylococci.** *J Clin Pathol* 1989, **42**:872-874.
72. Cegelski L, Pinkner JS, Hammer ND, Cusumano CK, Hung CS, Chourel E, Aberg V, Walker JN, Seed PC, Almqvist F, Chapman MR, Hultgren SJ: **Small-molecule inhibitors target *Escherichia coli* amyloid biogenesis and biofilm formation.** *Nat Chem Biol* 2009, **5**:913-919.
73. Oren A: **Population dynamics of Halobacteria in the Dead Sea water column.** *Limnol Oceanogr* 1983, **28**:1094-1103.
74. Anton J, Meseguer I, Rodriguez-Valera F: **Production of an extracellular polysaccharide by *Haloferax mediterranei*.** *Appl Environ Microbiol* 1988, **54**:2381-2386.
75. Zhao D, Cai L, Wu J, Li M, Liu H, Han J, Zhou J, Xiang H: **Improving polyhydroxyalkanoate production by knocking out the genes involved in exopolysaccharide biosynthesis in *Haloferax mediterranei*.** *Appl Microbiol Biotechnol* 2013, **97**:3027-3036.
76. Dominiak DM, Nielsen JL, Nielsen PH: **Extracellular DNA is abundant and important for microcolony strength in mixed microbial biofilms.** *Environ Microbiol* 2011, **13**:710-721.
77. Whitchurch CB, Tolker-Nielsen T, Ragas PC, Mattick JS: **Extracellular DNA required for bacterial biofilm formation.** *Science* 2002, **295**:1487.
78. Izano EA, Amarante MA, Kher WB, Kaplan JB: **Differential roles of poly-N-acetylglucosamine surface polysaccharide and extracellular DNA in *Staphylococcus aureus* and *Staphylococcus epidermidis* biofilms.** *Appl Environ Microbiol* 2008, **74**:470-476.
79. Chimileski S, Dolas K, Naor A, Gophna U, Papke RT: **Extracellular DNA metabolism in *Haloferax volcanii*.** *Front Microbiol* 2014, **5**:57.
80. Zerulla K, Chimileski S, Nather D, Gophna U, Papke RT, Soppa J: **DNA as a phosphate storage polymer and the alternative advantages of polyploidy for growth or survival.** *PLoS One* 2014, **9**:e94819.
81. DePas WH, Chapman MR: **Microbial manipulation of the amyloid fold.** *Res Microbiol* 2012, **163**:592-606.
82. Romero D, Sanabria-Valentin E, Vlamakis H, Kolter R: **Biofilm inhibitors that target amyloid proteins.** *Chem Biol* 2013, **20**:102-110.
83. Teather RM, Wood PJ: **Use of Congo red-polysaccharide interactions in enumeration and characterization of cellulolytic bacteria from the bovine rumen.** *Appl Environ Microbiol* 1982, **43**:777-780.
84. Plakoutis G, Taddei N, Stefani M, Chiti F: **Aggregation of the acylphosphatase from *Sulfolobus solfataricus*: the folded and partially unfolded states can both be precursors for amyloid formation.** *J Biol Chem* 2004, **279**:14111-14119.
85. Wei X, Pathak DT, Wall D: **Heterologous protein transfer within structured myxobacteria biofilms.** *Mol Microbiol* 2011, **81**:315-326.
86. Lu A, Cho K, Black WP, Duan XY, Lux R, Yang Z, Kaplan HB, Zusman DR, Shi W: **Exopolysaccharide biosynthesis genes required for social motility in *Myxococcus xanthus*.** *Mol Microbiol* 2005, **55**:206-220.
87. Kearns DB: **A field guide to bacterial swarming motility.** *Nat Rev Microbiol* 2010, **8**:634-644.
88. Sager B, Kaiser D: **Intercellular C-signaling and the traveling waves of *Myxococcus*.** *Genes Dev* 1994, **8**:2793-2804.
89. Shimkets LJ, Kaiser D: **Induction of coordinated movement of *Myxococcus xanthus* cells.** *J Bacteriol* 1982, **152**:451-461.
90. Tripepi M, Imam S, Pohlschroder M: ***Haloferax volcanii* flagella are required for motility but are not involved in PibD-dependent surface adhesion.** *J Bacteriol* 2010, **192**:3093-3102.
91. Tripepi M, Esquivel RN, Wirth R, Pohlschroder M: ***Haloferax volcanii* cells lacking the flagellin FlgA2 are hypermotile.** *Microbiology* 2013, **159**:2249-2258.
92. Zusman DR, Scott AE, Yang Z, Kirby JR: **Chemosensory pathways, motility and development in *Myxococcus xanthus*.** *Nat Rev Microbiol* 2007, **5**:862-872.
93. Oren A, Gurevich P: **Characterization of the dominant halophilic Archaea in a bacterial bloom in the dead sea.** *FEMS Microbiol Ecol* 1993, **12**:249-256.
94. Abdul Halim MF, Pfeiffer F, Zou J, Frisch A, Haft D, Wu S, Tolic N, Brewer H, Payne SH, Pasa-Tolic L, Pohlschroder M: ***Haloferax volcanii* archaeosortase is required for motility, mating, and C-terminal processing of the S-layer glycoprotein.** *Mol Microbiol* 2013, **88**:1164-1175.
95. Rosenshine I, Mevarech M: **The kinetics of the genetic exchange process in *Halobacterium volcanii* mating.** In *General and Applied Aspects of Halophilic Microorganisms*. Edited by Rodriguez-Valera F. New York: Plenum; 1991:265-270.
96. Nudelman E, Wall D, Kaiser D: **Cell-to-cell transfer of bacterial outer membrane lipoproteins.** *Science* 2005, **309**:125-127.

97. Schertzer JW, Whiteley M: **Bacterial outer membrane vesicles in trafficking, communication and the host-pathogen interaction.** *J Mol Microbiol Biotechnol* 2013, **23**:118–130.
98. Konovalova A, Sogaard-Andersen L: **Close encounters: contact-dependent interactions in bacteria.** *Mol Microbiol* 2011, **81**:297–301.
99. Norman TM, Lord ND, Paulsson J, Losick R: **Memory and modularity in cell-fate decision making.** *Nature* 2013, **503**:481–486.
100. Holmes ML, Dyll-Smith M: **A plasmid vector with a selectable marker for halophilic archaeobacteria.** *J Bacteriol* 1990, **172**:756–761.
101. Holze A, Fischer S, Heyer R, Schutz S, Zacharias M, Walther P, Allers T, Marchfelder A: **Maturation of the 5S rRNA 5' end is catalyzed *in vitro* by the endonuclease tRNase Z in the archaeon *H. volcanii*.** *RNA* 2008, **14**:928–937.
102. Charlebois RL, Lam WL, Cline SW, Doolittle WF: **Characterization of pHV2 from *Halobacterium volcanii* and its use in demonstrating transformation of an archaeobacterium.** *Proc Natl Acad Sci USA* 1987, **84**:8530–8534.
103. Cline SW, Lam WL, Charlebois RL, Schalkwyk LC, Doolittle WF: **Transformation methods for halophilic archaeobacteria.** *Can J Microbiol* 1989, **35**:148–152.
104. Puchtler H, Waldrop FS, Meloan SN: **A review of light, polarization and fluorescence microscopic methods for amyloid.** *Appl Pathol* 1985, **3**:5–17.
105. Westermark GT, Johnson KH, Westermark P: **Staining methods for identification of amyloid in tissue.** In *Methods in Enzymology*. 309th edition. Edited by Wetzel R, Abelson JN, Simon MI. Sheffield, UK: Academic; 1999:3–25.
106. Schindelin J, Arganda-Carreras I, Frise E, Kaynig V, Longair M, Pietzsch T, Preibisch S, Rueden C, Saalfeld S, Schmid B, Tinevez JY, White DJ, Hartenstein V, Eliceiri K, Tomancak P, Cardona A: **Fiji: an open-source platform for biological-image analysis.** *Nat Methods* 2012, **9**:676–682.

doi:10.1186/s12915-014-0065-5

Cite this article as: Chimileski et al.: Biofilms formed by the archaeon *Haloflex volcanii* exhibit cellular differentiation and social motility, and facilitate horizontal gene transfer. *BMC Biology* 2014 **12**:65.

Submit your next manuscript to BioMed Central and take full advantage of:

- Convenient online submission
- Thorough peer review
- No space constraints or color figure charges
- Immediate publication on acceptance
- Inclusion in PubMed, CAS, Scopus and Google Scholar
- Research which is freely available for redistribution

Submit your manuscript at
www.biomedcentral.com/submit

